

Semiclassical Approach to Competing Orders in Two-leg Spin Ladder with Ring-Exchange

K. Totsuka

Yukawa Institute for Theoretical Physics, Kyoto University, Kitashirakawa Oiwake-Cho, Kyoto 606-8502, Japan

P. Lecheminant

Laboratoire de Physique Théorique et Modélisation, CNRS UMR 8089, Université de Cergy-Pontoise, Site de Saint-Martin, 2 avenue Adolphe Chauvin, 95302 Cergy-Pontoise Cedex, France

S. Capponi

Laboratoire de Physique Théorique, Université de Toulouse, UPS (IRSAMC), F-31062 Toulouse, France and CNRS, LPT (IRSAMC), F-31062 Toulouse, France

We investigate the competition between different orders in the two-leg spin ladder with a ring-exchange interaction by means of a bosonic approach. The latter is defined in terms of spin-1 hardcore bosons which treat the Néel and vector chirality order parameters on an equal footing. A semiclassical approach of the resulting model describes the phases of the two-leg spin ladder with a ring-exchange. In particular, we derive the low-energy effective actions which govern the physical properties of the rung-singlet and dominant vector chirality phases. As a by-product of our approach, we reveal the mutual induction phenomenon between spin and chirality with, for instance, the emergence of a vector-chirality phase from the application of a magnetic field in bilayer systems coupled by four-spin exchange interactions.

PACS numbers: 75.10.Jm, 75.10.Pq

I. INTRODUCTION

Multiple-spin exchange interactions have attracted much interest for a long time. These interactions appear either as many-body direct exchange processes¹ or as higher-order corrections in the strong-coupling expansion of the half-filled Hubbard model.^{2,3} In most cases (especially in Mott insulators), the four-spin ring (or cyclic) exchange is rather small compared with the usual Heisenberg term. However, it may play a significant role in ³He, where hardcore repulsion makes many-body exchanges more likely than the standard two-body one, and Mott insulators close to the metal-insulator transitions. In fact, such interactions are expected to be crucial for explaining unusual magnetic behavior in ³He absorbed on graphite^{4,5}, Wigner crystals⁶ and some Mott insulators on triangular lattices.⁷ The relevance of the four-spin cyclic exchange has also been reported^{8–17} in fully describing the inelastic neutron-scattering experiments for such cuprates as La₂CuO₄, La₆Ca₈Cu₂₄O₄₁, La₄Ca₁₀Cu₂₄O₄₁, CaCu₂O₃, and SrCu₂O₃.

A second motivation to investigate multiple-spin exchange interactions stems from the exotic physics that emerges from their competition with the Heisenberg spin exchange. For instance, certain sorts of spin nematic phases are known to be stabilized in some two-dimensional Heisenberg magnets with ring-exchange interaction.^{18–20} Also multiple-spin exchanges can lead to new emerging quantum critical behaviors like the deconfined quantum criticality^{21,22} or the spin Bose-metal.²³ On top of these novel phases, even more exotic topological phases have been predicted to be realized with such interactions.^{24,25}

A paradigmatic and minimal model that realizes these two aspects of the multiple-spin exchange interactions would be

the two-leg spin ladder with a ring-exchange:

$$\mathcal{H} = J \sum_{r=\text{rungs}} (\mathbf{S}_{1,r} \cdot \mathbf{S}_{1,r+1} + \mathbf{S}_{2,r} \cdot \mathbf{S}_{2,r+1}) + J_{\perp} \sum_r \mathbf{S}_{1,r} \cdot \mathbf{S}_{2,r} + K_4 \sum_{\text{plaquettes}} (P_4 + P_4^{-1}), \quad (1)$$

where $\mathbf{S}_{a,r}$ ($a = 1, 2$) denotes the spin-1/2 operator on the chain- a and the rung r of the spin ladder. The parameters J and J_{\perp} respectively are the intrachain- and the interchain exchange coupling (Fig. 1 (a)). The ring exchange P_4 is defined on each plaquette (two-rung cluster: Fig. 1 (b)) and cyclically permutes the states of the four spins on the plaquette. This model is considered as relevant to describe the physical properties of ladder compounds e.g. La₄Ca₁₀Cu₂₄O₄₁ (Refs. 9 and 10) and CaCu₂O₃ (Ref. 16). The model (1) is interesting in its own right and has been studied extensively over the years and its phase diagram^{26–30}, ground-state- and dynamical properties^{14,31–33}, quantum phase transitions^{34–36}, and entanglement properties^{37–39} have been explored by both analytical and numerical approaches.

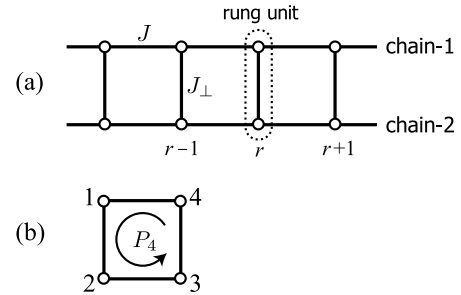


FIG. 1. Two-leg ladder (a) and four-spin plaquette (b) on which ring-exchange P_4 is defined.

The zero-temperature phase diagram is rich and six different phases have been identified²⁷: the ferromagnetic phase, the rung-singlet (RS) phase, the staggered dimerized phase, the scalar chirality phase, the dominant vector chirality (VC) phase, and the dominant collinear spin phase. All phases are gapful except the ferromagnetic phase. The four-spin cyclic exchange manifests itself by stabilizing the scalar chirality phase, which spontaneously breaks the time-reversal symmetry, and the VC phase. The latter phase has a unique singlet ground state with a finite gap. In sharp contrast to the usual RS phase of the two-leg spin ladder, the lowest triplet excitation of the VC phase is not the standard triplon created by the spin operators $\mathbf{S}_{a,r}$ but is built from the vector chirality $\mathbf{S}_{1,r} \times \mathbf{S}_{2,r}$ as we will show below. Consequently, the dominant ground-state correlations of this phase occur not in the spin-spin channel but rather in the vector-chirality channel.^{27,28} The relationship between the RS and VC phases can be simply understood by means of a spin-chirality duality transformation.^{28,29} Under the transformation

$$\begin{aligned}\mathbf{S}_{1,r} &\rightarrow \frac{1}{2}(\mathbf{S}_{1,r} + \mathbf{S}_{2,r}) - \mathbf{S}_{1,r} \times \mathbf{S}_{2,r} \\ \mathbf{S}_{2,r} &\rightarrow \frac{1}{2}(\mathbf{S}_{1,r} + \mathbf{S}_{2,r}) + \mathbf{S}_{1,r} \times \mathbf{S}_{2,r},\end{aligned}\quad (2)$$

the Néel staggered magnetization $\mathbf{S}_{1,r} - \mathbf{S}_{2,r}$ is interchanged with the VC order parameter $2\mathbf{S}_{1,r} \times \mathbf{S}_{2,r}$ and vice-versa.^{28,29} Model (1) is invariant, i.e. self-dual, under the duality transformation (2) when $K_4 = J/2$. Physics in the vicinity of this point is dictated by the competition between the RS and the VC orders.

In this paper, we investigate the competition between these orders by means of a semiclassical approach which treats the Néel antiferromagnetic (NAF) and the VC order parameters on an equal footing. To this end, the model (1) is first expressed in terms of spin-1 hardcore boson operators that create triplet states out of the vacuum.⁴⁰ In this basis, the spin-chirality transformation (2) has a simple interpretation as the U(1) gauge transformation of the bosons.³⁶ The next step of the approach is to perform a simple mean-field approximation of the phases of the bosonic model. We then incorporate quantum fluctuations by constructing semiclassical low-energy Hamiltonians which describe the competition of the RS and the VC orders as well as the usual rotational fluctuations. It is important to observe that our approach is not restricted to one dimension but applies to e.g. higher-dimensional systems consisting of two-spin clusters as well. In this respect, the approach is directly relevant to two-dimensional half-filled bilayer spin-1/2 fermions with ring-exchange interaction.⁴¹ Finally, we investigate the interesting mutual induction phenomenon between spin and chirality degrees of freedom within our semiclassical approach which signals, for instance, the emergence of a VC phase by the application of a magnetic field. This last result has been first predicted in one dimension by means of the bosonization approach.⁴²

The rest of the paper is organized as follows. In Sec. II, the mapping of model (1) onto that of spin-1 hardcore bosons and the path-integral representation of the resulting model,

on which our semiclassical approach is based, are presented. Then, we draw the semiclassical phase diagram in Sec. III by minimizing the classical energy, which is equivalent to mean-field approximation. The low-energy effective actions for the main phases are then derived in Sec. IV. As an application of our method, we investigate the mutual induction phenomenon between spin and chirality in Sec. V. Finally, our concluding remarks are presented in Sec. VI. The paper is supplied with one appendix which provides some technical information on the semiclassical approach.

II. EFFECTIVE SPIN-1 HARDCORE BOSONS APPROACH

In this section, we introduce three hardcore bosons to map the model (1) onto an effective spin-1 boson Hamiltonian. This approach will enable us to illustrate how competition among different orders (specifically, antiferromagnetic (AF) order and chiral one) is described in our framework.

A. Dimer basis and spin-chirality rotation

First we begin with analyzing the Hilbert space of each rung which is an obvious unit of construction. In describing the states on each rung, it is convenient to move from the standard spin-1/2 (\uparrow/\downarrow) basis to the singlet-triplet basis:

$$\begin{aligned}|s\rangle &= \frac{1}{\sqrt{2}}(|\uparrow\downarrow\rangle - |\downarrow\uparrow\rangle) \\ |t_x\rangle &= -\frac{1}{\sqrt{2}}(|\uparrow\uparrow\rangle - |\downarrow\downarrow\rangle), \quad |t_y\rangle = \frac{i}{\sqrt{2}}(|\uparrow\uparrow\rangle + |\downarrow\downarrow\rangle) \\ |t_z\rangle &= \frac{1}{\sqrt{2}}(|\uparrow\downarrow\rangle + |\downarrow\uparrow\rangle).\end{aligned}\quad (3)$$

These four states may be thought of as created by the following four (constrained) bosons obeying the standard bosonic commutation relations:⁴⁰

$$\begin{aligned}|s\rangle &= s^\dagger|0\rangle, \quad |t_\alpha\rangle = t_\alpha^\dagger|0\rangle \quad (\alpha = x, y, z) \\ s^\dagger s + \sum_{\alpha=x,y,z} t_\alpha^\dagger t_\alpha &= 1.\end{aligned}\quad (4)$$

For our purpose, however, it is more convenient to identify $|s\rangle$ with the empty state (boson vacuum) and represent the remaining triplet states by using three *hardcore* bosons b_α

$$|0\rangle_{\text{hcb}} \equiv |s\rangle, \quad b_\alpha^\dagger|0\rangle_{\text{hcb}} \equiv |t_\alpha\rangle \quad (5)$$

obeying the following nonstandard commutation relations:

$$[b_{r,\alpha}, b_{r',\beta}^\dagger] = \left\{ \delta_{\alpha\beta} (1 - n_r^B) - b_{r,\beta}^\dagger b_{r,\alpha} \right\} \delta_{r,r'}, \quad (6)$$

with n_B being the number operator of the hardcore boson:

$$n_r^B \equiv \sum_{\alpha=x,y,z} b_{r,\alpha}^\dagger b_{r,\alpha} = \mathbf{S}_{1,r} \cdot \mathbf{S}_{2,r} + 3/4. \quad (7)$$

The crucial step is to realize that under the hardcore constraint

$$n_r^B = 0, 1, \quad (8)$$

the boson creation operator can be represented by a complex combination of two different order parameters:³⁶

$$b_{r,\alpha}^\dagger = \frac{1}{2}(\mathbf{S}_{1,r} - \mathbf{S}_{2,r})^\alpha + i(\mathbf{S}_{1,r} \times \mathbf{S}_{2,r})^\alpha \quad (\alpha = x, y, z). \quad (9)$$

From this equation, one sees that the competition between the AF fluctuations (carried by $(\mathbf{S}_{1,r} - \mathbf{S}_{2,r})$) and the (vector) chiral ones ($(\mathbf{S}_{1,r} \times \mathbf{S}_{2,r})$) is implemented in a single bosonic object b in a unifying way. Also, it is easy to see that (spin-independent) gauge transformation $b_\alpha^\dagger \mapsto e^{i\varphi} b_\alpha^\dagger$ translates into an SO(2) rotation (*spin-chirality rotation*²⁹) for the order-parameter doublet $(\mathbf{S}_{1,r} - \mathbf{S}_{2,r}, \mathbf{S}_{1,r} \times \mathbf{S}_{2,r})$:

$$\begin{pmatrix} \mathbf{S}_1 - \mathbf{S}_2 \\ 2\mathbf{S}_1 \times \mathbf{S}_2 \end{pmatrix} \mapsto \begin{pmatrix} \cos \varphi & -\sin \varphi \\ \sin \varphi & \cos \varphi \end{pmatrix} \begin{pmatrix} \mathbf{S}_1 - \mathbf{S}_2 \\ 2\mathbf{S}_1 \times \mathbf{S}_2 \end{pmatrix}. \quad (10)$$

In particular, the spin-chirality duality transformation (2) can be obtained from Eq. (10) with $\varphi = \pi/2$.

B. Generalized boson Hubbard model

It is convenient to rewrite the model Hamiltonian (1) in terms of the hardcore boson introduced above. In terms of the bosonic operators $b_{r,\alpha}$, the (spin) Hamiltonian (1) can be mapped onto the following spin-1 Bose-Hubbard model:³⁶

$$\begin{aligned} \mathcal{H} = & t \sum_{r,\alpha} \left(b_{r,\alpha}^\dagger b_{r+1,\alpha} + b_{r+1,\alpha}^\dagger b_{r,\alpha} \right) \\ & + u \sum_{r,\alpha} \left(b_{r,\alpha}^\dagger b_{r+1,\alpha}^\dagger + b_{r+1,\alpha} b_{r,\alpha} \right) \\ & + \sum_r \left[J_{\text{bl}} \mathbf{T}_r \cdot \mathbf{T}_{r+1} + J_{\text{bq}} (\mathbf{T}_r \cdot \mathbf{T}_{r+1})^2 \right] \\ & + V_c \sum_r n_r^B n_{r+1}^B - \mu \sum_r n_r^B. \end{aligned} \quad (11)$$

The spin \mathbf{T} of the hardcore boson b is given by

$$\mathbf{T}_{r,\alpha} \equiv -i \epsilon_{\alpha\beta\gamma} b_{r,\beta}^\dagger b_{r,\gamma} \quad (12)$$

where the projection onto the occupied (i.e. $n^B \neq 0$) states is implied on both sides. The ring-exchange model (1) is reproduced if we choose:

$$\begin{aligned} t = \frac{1}{2}J + K_4, \quad u = \frac{1}{2}J - K_4, \quad J_{\text{bl}} = \frac{1}{2}J + K_4, \\ J_{\text{bq}} = 0, \quad V_c = 4K_4, \quad \mu = 4K_4 - J_\perp. \end{aligned} \quad (13)$$

Note that the Hamiltonian (11) is the most general one allowed by the requirements of (i) SU(2) symmetry, (ii) time-reversal invariance, (iii) exchange of the two chains ($1 \leftrightarrow 2$) and (iv) short-range interactions (i.e. interactions only involve two adjacent rungs). In this respect, model (11) describes two-leg spin ladder with general four-spin exchange interactions.³⁶

The ring-exchange is special in the sense that there is no bi-quadratic exchange interaction: $J_{\text{bq}} = 0$. It is also important to note that the U(1) gauge-symmetry for the bosons, i.e. the spin-chirality rotation (10), is *explicitly* broken unless $u = 0$. The spin-chirality duality symmetry (2) transforms the pairing term as: $u \mapsto -u$. In the self-dual case, i.e. $u = 0$, model (11) is directly relevant to spinor Bose quantum gases with hyperfine spin $F = 1$ loaded into an optical lattice.⁴³

In the following sections, we develop a semiclassical approach to discuss the physical properties of various phases of the model (1) (or the equivalent model (11)). In particular, we are interested in the two non-magnetic phases^{27,28} (dubbed ‘rung singlet’ and ‘dominant vector chirality’ in Ref. 27). The effective models derived in Sec. IV provide us with a simple and natural framework of describing the competition of spin and chirality degrees of freedom.

C. Coherent-state-construction of path-integral

As usual, the starting point of the path-integral approach is the construction of the many-body coherent state basis for the two-leg ladder model with a ring-exchange (1) and the spin-1 boson Hubbard model (11). In this respect, let us consider spin-1 hardcore bosons b_α^\dagger ($\alpha = x, y, z$) on a unit of construction (e.g. a rung in the case of the two-leg ladder). As has been mentioned in Sec. II A, these boson operators are parametrized in terms of the two competing (real) order parameters $\hat{\mathbf{q}}$ and $\hat{\mathbf{p}}$:

$$b_{r,\alpha}^\dagger = (\hat{\mathbf{q}}_r)_\alpha + i(\hat{\mathbf{p}}_r)_\alpha \quad (\alpha = x, y, z), \quad (14)$$

where in our ladder problem, $(\hat{\mathbf{q}}_r)_\alpha$ and $(\hat{\mathbf{p}}_r)_\alpha$ are respectively the staggered magnetization and the vector-chiral order parameter:

$$\hat{\mathbf{q}}_r = \frac{1}{2}(\mathbf{S}_{1,r} - \mathbf{S}_{2,r}), \quad \hat{\mathbf{p}}_r = \mathbf{S}_{1,r} \times \mathbf{S}_{2,r} \quad (15)$$

(see Eq. (9)).

Clearly, arbitrary states on each unit can be represented as:⁴⁴

$$|\psi\rangle = s|s\rangle + \sum_{\alpha=x,y,z} t_\alpha |t_\alpha\rangle \equiv |s, \mathbf{t}\rangle, \quad (16)$$

where

$$s^* s + \mathbf{t}^* \cdot \mathbf{t} = 1, \quad (17)$$

is required by the normalization condition. Since the overall phase is irrelevant, we may fix the gauge in such a way that the singlet amplitude s is real and positive:

$$s = \sqrt{1 - \mathbf{t}^* \cdot \mathbf{t}} \quad (\mathbf{t}^* \cdot \mathbf{t} \leq 1) \quad (18)$$

and parametrize the complex vector \mathbf{t} in terms of two *real* vectors \mathbf{A} and \mathbf{B} as:

$$\begin{aligned} \mathbf{t} \equiv \mathbf{A} - i\mathbf{B}, \quad s = \sqrt{1 - (\mathbf{A} \cdot \mathbf{A} + \mathbf{B} \cdot \mathbf{B})} \\ (\mathbf{A}, \mathbf{B} \in \mathbb{R}^3, \mathbf{A} \cdot \mathbf{A} + \mathbf{B} \cdot \mathbf{B} \leq 1). \end{aligned} \quad (19)$$

One of the greatest merits of using this representation is that the two order parameters $\hat{\mathbf{q}}$ and $\hat{\mathbf{p}}$, which are related to the boson by Eq. (14), are expressed simply by \mathbf{A} and \mathbf{B} :

$$\langle s, \mathbf{t} | \hat{\mathbf{q}} | s, \mathbf{t} \rangle = (s^* \mathbf{t} + \mathbf{t}^* s) / 2 = \sqrt{1 - (\mathbf{A}^2 + \mathbf{B}^2)} \mathbf{A} \quad (20a)$$

$$\langle s, \mathbf{t} | \hat{\mathbf{p}} | s, \mathbf{t} \rangle = i(s^* \mathbf{t} - \mathbf{t}^* s) / 2 = \sqrt{1 - (\mathbf{A}^2 + \mathbf{B}^2)} \mathbf{B}. \quad (20b)$$

From these equations, it is obvious that the spin-chirality rotation (10) is equivalent to the *gauge transformation* of the triplet operators \mathbf{t}

$$\mathbf{t}^* \mapsto e^{i\varphi} \mathbf{t}^* \quad (21)$$

or the following O(2) transformation for the pair (\mathbf{A}, \mathbf{B}) :

$$\begin{pmatrix} \mathbf{A} \\ \mathbf{B} \end{pmatrix} \mapsto \begin{pmatrix} \cos \varphi & -\sin \varphi \\ \sin \varphi & \cos \varphi \end{pmatrix} \begin{pmatrix} \mathbf{A} \\ \mathbf{B} \end{pmatrix}. \quad (22)$$

In the case of the two-leg ladder where the triplet boson is defined on the rung, the pair of order parameters is given by Eq. (9) and the above is nothing but the spin-chirality transformation (10).²⁸

The magnetic moment \mathbf{T} , that generates the O(3) rotation of the boson triplet, is expressed as (see Eq. (12)):

$$\langle s, \mathbf{t} | \hat{\mathbf{T}} | s, \mathbf{t} \rangle = -i(\mathbf{t}^* \times \mathbf{t}) = -2(\mathbf{A} \times \mathbf{B}). \quad (23)$$

If we take a single rung as the unit in the case of the two-leg ladder, $\hat{\mathbf{T}} = \mathbf{S}_1 + \mathbf{S}_2$. The boson density is another important quantity and takes the following expression:

$$\langle s, \mathbf{t} | n^B | s, \mathbf{t} \rangle = \mathbf{t}^* \cdot \mathbf{t} = (\mathbf{A}^2 + \mathbf{B}^2). \quad (24)$$

The many-body coherent state basis are constructed as the tensor-product of the local coherent states:

$$\bigotimes_r |s_r, \mathbf{t}_r\rangle = \bigotimes_r |\mathbf{A}_r, \mathbf{B}_r\rangle. \quad (25)$$

With these expressions, we can write down the desired path-integral formula for many-spin systems⁴⁴ by following the standard steps:^{45,46}

$$\mathcal{S} = \int dt \sum_r (\mathbf{A}_r \cdot \partial_t \mathbf{B}_r - \mathbf{B}_r \cdot \partial_t \mathbf{A}_r) - \int dt \mathcal{H}_{\text{cl}}(\{\mathbf{A}\}, \{\mathbf{B}\}), \quad (26)$$

where \mathcal{H}_{cl} is given by the expectation value of the Hamiltonian with respect to the many-body coherent state $\bigotimes_r |s_r, \mathbf{t}_r\rangle$. In obtaining \mathcal{H}_{cl} , the easiest way is to use the spin-1 Bose-Hubbard model (11) with the coupling constants (13) and then plug the following expressions:

$$\begin{aligned} b_{r,\alpha}^\dagger &\mapsto \sqrt{1 - (\mathbf{A}_r^2 + \mathbf{B}_r^2)} (\mathbf{A}_r + i \mathbf{B}_r), \\ b_{r,\alpha} &\mapsto \sqrt{1 - (\mathbf{A}_r^2 + \mathbf{B}_r^2)} (\mathbf{A}_r - i \mathbf{B}_r). \end{aligned} \quad (27)$$

The final result reads as follows:

$$\mathcal{H}_{\text{cl}} = \mathcal{H}_{\text{magnetic}} + \mathcal{H}_{\text{hopping}} + \mathcal{H}_{\text{charge}} \quad (28a)$$

$$\begin{aligned} \mathcal{H}_{\text{magnetic}} &\equiv (2J + 4K_4) \sum_r \{ (\mathbf{A}_r \cdot \mathbf{A}_{r+1})(\mathbf{B}_r \cdot \mathbf{B}_{r+1}) \\ &\quad - (\mathbf{A}_r \cdot \mathbf{B}_{r+1})(\mathbf{B}_r \cdot \mathbf{A}_{r+1}) \}, \end{aligned} \quad (28b)$$

$$\begin{aligned} \mathcal{H}_{\text{hopping}} &\equiv \sum_r 4\sqrt{1 - (\mathbf{A}_r^2 + \mathbf{B}_r^2)} \sqrt{1 - (\mathbf{A}_{r+1}^2 + \mathbf{B}_{r+1}^2)} \\ &\quad \times \left\{ \frac{J}{2} \mathbf{A}_r \cdot \mathbf{A}_{r+1} + K_4 \mathbf{B}_r \cdot \mathbf{B}_{r+1} \right\}, \end{aligned} \quad (28c)$$

$$\begin{aligned} \mathcal{H}_{\text{charge}} &\equiv (J_\perp + 2K_4) \sum_r \left\{ (\mathbf{A}_r^2 + \mathbf{B}_r^2) - \frac{3}{4} \right\} \\ &\quad + 4K_4 \sum_r \left\{ (\mathbf{A}_r^2 + \mathbf{B}_r^2) - \frac{3}{4} \right\} \left\{ (\mathbf{A}_{r+1}^2 + \mathbf{B}_{r+1}^2) - \frac{3}{4} \right\}. \end{aligned} \quad (28d)$$

The magnetic- and the charge part are invariant under the spin-chirality U(1) transformation (10) and the competition between the (π, π) antiferromagnetic correlation (\mathbf{A}) and the chirality correlation (\mathbf{B}) is controlled solely by the two coupling constants in $\mathcal{H}_{\text{hopping}}$:

$$J_A \equiv \frac{t+u}{2} = \frac{J}{2}, \quad J_B \equiv \frac{t-u}{2} = K_4. \quad (29)$$

III. MEAN-FIELD PHASE DIAGRAM

In this section, we determine the classical ground state of the model (1) or its bosonic equivalent (11), on the basis of which we develop the effective field theories in Sec. IV.

A. General properties

Before presenting the results, we describe the relationship between the obtained $\{\mathbf{A}, \mathbf{B}\}$ -configurations and the physical phases. By construction, it is obvious that our calculation is nothing but the mean-field approximation for the spin-1 boson using the following product state:

$$\begin{aligned} |\Psi\rangle_{\{\eta_r, \mathbf{a}_r, \mathbf{b}_r\}} &= \bigotimes_r \left\{ \cos \frac{\eta_r}{2} |s\rangle + \sin \frac{\eta_r}{2} \sum_{\alpha=x,y,z} (\mathbf{a} - i \mathbf{b})_{r,\alpha} |t_{r,\alpha}\rangle \right\}, \end{aligned} \quad (30)$$

where we have introduced

$$s_r = \cos \frac{\eta_r}{2}, \quad \mathbf{t}_r^* = \mathbf{A}_r + i \mathbf{B}_r = \sin \frac{\eta_r}{2} (\mathbf{a}_r + i \mathbf{b}_r), \quad (31)$$

with $\mathbf{a}_r^2 + \mathbf{b}_r^2 = 1$. The parameter η_r ($0 \leq \eta_r \leq \pi$) controls the local boson density n_B through the relation

$$\langle \Psi | n_r^B | \Psi \rangle_{\{\eta_r, \mathbf{a}_r, \mathbf{b}_r\}} = \sin^2 \frac{\eta_r}{2}. \quad (32)$$

As has been mentioned in the previous section, the spin-1 (hardcore) boson operators are parametrized in terms of the two competing (real) order parameters $\hat{\mathbf{q}}$ and $\hat{\mathbf{p}}$ (see Eq. (14)). One can then compute the expectation values of these operators in the coherent state (30):

$$\begin{aligned} \langle \Psi | \hat{q}_{r,\alpha} | \Psi \rangle_{\{\eta_r, \mathbf{a}_r, \mathbf{b}_r\}} &= \left\langle \frac{1}{2} (\mathbf{S}_1 - \mathbf{S}_2)^\alpha \right\rangle = \frac{1}{2} \sin \eta_r (\mathbf{a}_r)_\alpha, \\ \langle \Psi | \hat{p}_{r,\alpha} | \Psi \rangle_{\{\eta_r, \mathbf{a}_r, \mathbf{b}_r\}} &= \langle (\mathbf{S}_1 \times \mathbf{S}_2)^\alpha \rangle = \frac{1}{2} \sin \eta_r (\mathbf{b}_r)_\alpha. \end{aligned} \quad (33)$$

Therefore, the phases with $\eta_r \neq 0, \pi$ in general correspond to superfluids in that $\langle b_{r,a}^\dagger \rangle \neq 0$.

Information on magnetism may be obtained by the spin-1 magnetic moment (12) on each rung:

$$\langle \Psi | \mathbf{T}_r | \Psi \rangle_{\{\eta_r, \mathbf{a}_r, \mathbf{b}_r\}} = \langle \mathbf{S}_1 + \mathbf{S}_2 \rangle = -2 \sin^2 \frac{\eta_r}{2} \mathbf{a}_r \times \mathbf{b}_r. \quad (34)$$

From Eqs. (33) and (34), it is obvious that if, for some reasons, the system chooses the state with $\mathbf{a} = \mathbf{0}$, $\mathbf{b} \neq \mathbf{0}$ ($\eta \neq 0, \pi$), a moment free (i.e. $\langle \mathbf{S}_1 + \mathbf{S}_2 \rangle = \langle \mathbf{S}_1 - \mathbf{S}_2 \rangle = \mathbf{0}$) chiral phase $\langle \mathbf{S}_{1,r} \times \mathbf{S}_{2,r} \rangle \neq \mathbf{0}$ (*p*-type spin-nematic⁴⁷) is realized. Similarly, $\mathbf{a} \neq \mathbf{0}$, $\mathbf{b} = \mathbf{0}$ implies another type of phases with collinear spin order (either (π, π) or $(0, \pi)$).

Since we are dealing with spin-1 bosons, we may expect (typically for large enough biquadratic interaction J_{bq}) a phase characterized by the following rank-2 tensor (*spin-nematic phase*) to occur:

$$Q_r^{\alpha\beta} \equiv \frac{1}{2} (T_r^\alpha T_r^\beta + T_r^\beta T_r^\alpha) - \frac{1}{3} \delta^{\alpha\beta} \mathbf{T}_r^2. \quad (35)$$

In the mean-field state (30), the above tensor order parameter takes the value:

$$\begin{aligned} \langle \Psi | Q_r^{\alpha\beta} | \Psi \rangle_{\{\eta_r, \mathbf{a}_r, \mathbf{b}_r\}} \\ = -\sin^2 \frac{\eta_r}{2} \left\{ (\mathbf{a}_r)_\alpha (\mathbf{a}_r)_\beta + (\mathbf{b}_r)_\alpha (\mathbf{b}_r)_\beta - \frac{1}{3} \delta^{\alpha\beta} \right\}. \end{aligned} \quad (36)$$

When \mathbf{a} and \mathbf{b} are parallel to each other, the spin sector is in general spin-nematic with vanishing magnetic moment $\langle \mathbf{T} \rangle = \mathbf{0}$. Note that the two $\langle \mathbf{T} \rangle = \mathbf{0}$ phases described above have finite $\langle Q^{\alpha\beta} \rangle$ and that, in a sense, they may be thought of as spin-nematic. The only difference between spin-1 nematic and the other two states comes from the filling-dependent overall factors $\sin \eta$ and $\sin^2(\eta/2)$; the former can exist even in the spin-1 limit $\eta = \pi$ while the latter are not.

The charge part (Eq. (28d)) dictates the charge density distribution. For instance, for sufficiently large (positive) μ , the density saturates $n_B = 1$ and the system reduces to the (localized) spin-1 chain. For large enough V_c , on the other hand, the system may develop inhomogeneity, i.e. form a charge-density wave with alternating $n_B = 0$ and $n_B = 1$.

The general mean-field phase diagram, which results from these equations, will be presented elsewhere.⁴⁸ Here, we only stress that the set of coupling constants (t, u) is crucial for the competition between antiferromagnetism and chirality. To see this, we first calculate the kinetic energy by using the mean-field ansatz (30):

$$\begin{aligned} &\left\langle t \sum_{r,\alpha} \left(b_{r,\alpha}^\dagger b_{r+1,\alpha} + b_{r+1,\alpha}^\dagger b_{r,\alpha} \right) \right\rangle \\ &+ \left\langle u \sum_{r,\alpha} \left(b_{r,\alpha}^\dagger b_{r+1,\alpha}^\dagger + b_{r+1,\alpha} b_{r,\alpha} \right) \right\rangle \\ &= \sum_r \sin \eta_r \sin \eta_{r+1} \{ J_A \mathbf{a}_r \cdot \mathbf{a}_{r+1} + J_B \mathbf{b}_r \cdot \mathbf{b}_{r+1} \}, \end{aligned} \quad (37)$$

where the two couplings, that characterize the anisotropy in the spin-chirality space, are given by Eq. (29). For $u \neq 0$ and $\eta \neq 0, \pi$, an anisotropic superfluid forms; \mathbf{a}_r ($\propto \text{Re}(t_r^*)$) is dominant when $|J_A| > |J_B|$, while \mathbf{b}_r ($\propto \text{Im}(t_r^*)$) is dominant when $|J_A| < |J_B|$.

So far, we have presented the mean-field description of the phases of the spin-1 boson model. However, in one dimension, strong quantum fluctuations may destroy the ordered states predicted by the mean-field theory. In fact, as we will show in the next section by using low-energy effective theories, some of the ordered phases are replaced by gapped short-range phases which do not break rotational symmetry.

B. Two-leg ladder

The semiclassical ground state of the model (1) (or equivalently, (11)) is obtained by minimizing the energy functional $\mathcal{H}_{\text{cl}}(\{\mathbf{A}\}, \{\mathbf{B}\})$ in (28a) with respect to the variational parameters $\{\mathbf{A}_r\}$ and $\{\mathbf{B}_r\}$. As we have already seen, this is nothing but the mean-field treatment using (30). The resulting phase diagram contains six phases: (i) ‘NAF-dominant’, (ii) ‘chirality-dominant’, (iii) ‘partial-AF’, (iv) ‘F-nematic’, (v) ‘ferromagnetic’ and (vi) ‘singlet-product’. It is convenient to parametrize the coupling constants as:

$$J = \cos \theta, \quad K_4 = \sin \theta \quad (-\pi < \theta \leq \pi) \quad (38)$$

and map out the phase diagram as a function of θ (see Fig. 2).

Let us describe the nature of the six phases.

(i) *NAF-dominant*: This phase is described by $\mathbf{A}_r \neq \mathbf{0}$ and $\mathbf{B}_r = \mathbf{0}$. The resulting phase is characterized by vanishing (total) magnetic moment on each rung $\langle \mathbf{S}_1 + \mathbf{S}_2 \rangle = -2\mathbf{A} \times \mathbf{B}$ and *anti-parallel* ordering of \mathbf{A} (local chirality $\mathbf{B} = \mathbf{0}$). At the mean-field level, the symmetry $\text{SU}(2) \times \mathbb{Z}_2$ of the model (1) is broken down to $\text{SO}(2)$ (rotation around the ordered \mathbf{A}). Since \mathbf{A} corresponds to $\mathbf{S}_1 - \mathbf{S}_2$, the staggered order of \mathbf{A} implies the standard (π, π) Néel-ordered phase.

(ii) *chirality dominant*: The second phase is the dual ($\mathbf{A} \leftrightarrow \mathbf{B}$) of the former with $\mathbf{A}_r = \mathbf{0}$ and $\mathbf{B}_r \neq \mathbf{0}$. This phase has the same symmetry as the first phase and is non-magnetic (i.e. $\langle \mathbf{S}_1 \rangle = \langle \mathbf{S}_2 \rangle = \mathbf{0}$). However, the long-range order occurs in the chirality channel $\mathbf{B} \sim \mathbf{S}_1 \times \mathbf{S}_2$ in a staggered manner. The transition from the first phase occurs at the so-called self-dual

point $\theta = \theta_{sd} \equiv \tan^{-1}(1/2) \approx 0.1476\pi$ where $J_A = J_B$ (see Eq. (29)).

(iii) *partial-AF*: At $\theta = \pi/2$, the system begins to have a small local magnetization $\langle \mathbf{S}_1 + \mathbf{S}_2 \rangle$ on each rung and this partial magnetization orders in an AF manner. Note that both \mathbf{A} and \mathbf{B} take finite values in this phase. Within the semiclassical treatment, the energy of the partial-AF phase is very close to that of the chirality-dominant phase suggesting the instability of the former against quantum fluctuations.

(iv) *F-nematic*: At $\theta = \cos^{-1}(-2/\sqrt{5}) = \pi - \theta_{sd} \approx 0.8524\pi$ ($t = J_{bl} = J/2 + K_4 = 0$), the system enters a new non-magnetic phase which is similar to the first one ('NAF-dominant') except that now the \mathbf{A} fields align in a *parallel* (ferromagnetic) manner. If we regard the triplet state on each rung as an effective spin-1 state, this is nothing but the spin-nematic state (one can easily check $\langle \mathbf{T} \rangle = \mathbf{0}$, $Q^{\alpha\beta} \neq 0$) where \mathbf{A} plays the role of the director. This is why the name 'F-nematic' ('F' denotes *ferro*) is used here.

(v) *ferromagnetic*: For $\theta > \cos^{-1}\left(-\sqrt{\frac{32(36+\sqrt{7})}{1289}}\right) \approx 0.9354\pi$, the system is fully-occupied by the spin-1 states (i.e. $n_B = \mathbf{A}^2 + \mathbf{B}^2 = 1$) and these spin-1s form a polarized ferromagnetic state as a whole.

(vi) *singlet-product*: At $\theta = -\cos^{-1}(2/\sqrt{13}) \approx -0.3128\pi$ (where $3J + 2K_4 = 0$), the system becomes non-magnetic again through a first-order transition. Contrary to the ferromagnetic phase, all rungs are occupied by the singlet (i.e. $n_B = \mathbf{A}^2 + \mathbf{B}^2 = 0$) in the new phase. In terms of the original spin-1/2 ladder model, this is nothing but the singlet-product state (rung-singlet). The original symmetry $SU(2) \times \mathbb{Z}_2$ is not broken at all. In fact, a simple fluctuation analysis shows that the low-energy excitation is the gapped triplet. The singlet-product phase persists until the system enters the 'NAF-dominant' phase at $\theta = -\tan^{-1}(1/4) \approx -0.0780\pi$ (i.e. $J + 4K_4 = 0$), where the triplet gap vanishes.

The emergence of spin-nematic phase ('F-nematic') in the absence of biquadratic interaction J_{bq} (see Eq. (13)) may look surprising. However, this can be understood within the simple mean-field argument presented here. First we note that $J_{bl} = J/2 + K_4 > 0$ (< 0) for $\theta < \pi - \theta_{sd}$ ($\theta > \pi - \theta_{sd}$). In the region where we have 'F-nematic', the magnetic coupling $J_{bl} = J/2 + K_4 (< 0)$ is small and the chirality coupling $J_B = K_4 = \sin \theta$ is always positive (hence anti-parallel configuration of \mathbf{B} is favored), while the NAF-coupling $J_A = J/2 = \cos \theta/2$ is negative. In the 'partial-AF' phase, the system tends to develop weak local moments \mathbf{T} which align in an AF-manner to optimize the positive magnetic coupling J_{bl} ; the combination ($J_A < 0$, $J_B > 0$) stabilizes the parallel \mathbf{A} and the anti-parallel \mathbf{B} as the optimal configuration.

In the 'F-nematic' phase, on the other hand, the negative J_{bl} naively favors ferromagnetic alignment of the local moments \mathbf{T} . However, to realize it, configurations with (\mathbf{A} -parallel, \mathbf{B} -parallel) or (\mathbf{A} -antiparallel, \mathbf{B} -antiparallel) are needed and they are inconsistent with the signs of J_A and J_B (hence frustrated). Since $-J_A > J_B (> 0)$ and $|J_{bl}| \ll 1$, the system lowers the energy by choosing a non-magnetic state ('F-nematic') with *ferromagnetic* ordering of \mathbf{A} ($\mathbf{B} = \mathbf{0}$).

If we further increase θ , J_{bl} gets larger while the chiral-

ity coupling J_B becomes negligibly small. Then, the energy gain by forming a ferromagnetic (i.e. parallel \mathbf{T}) configuration overcomes the energy cost coming from the frustration in the \mathbf{B} -channel (i.e. parallel- \mathbf{B} for positive J_B) and hence the ferromagnetic state is stabilized.

So far, we have presented the mean-field description of the phases of the spin-1 boson model and found that in some of these phases, rotational symmetry is spontaneously broken at the mean-field level. However, in one dimension, strong quantum fluctuations may destroy the ordered states predicted by the mean-field theory. In fact, as we will show in the next section by using effective field theories, some of the ordered phases are replaced by gapped short-range phases which do not break rotational symmetry.

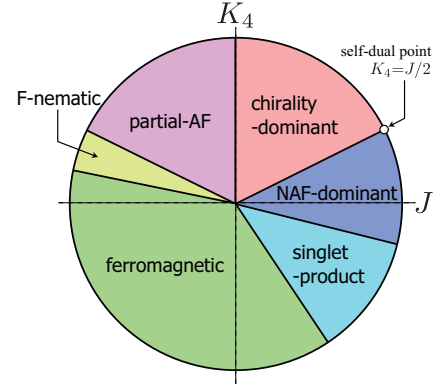


FIG. 2. (color online) Phase diagram of the model (1) ($J = \cos \theta$, $K_4 = \sin \theta$) obtained by applying a mean-field approximation to \mathcal{H}_{cl} (28a). The self-dual point ($K_4 = J/2$) separates the 'NAF-dominant' (i.e. \mathbf{A} -ordered) phase and the 'chirality-dominant' (\mathbf{B} -ordered) one. In (1+1)-D, strong quantum fluctuations turn these ordered phases into short-ranged ones.

IV. LOW-ENERGY EFFECTIVE ACTIONS

Having established the mean-field phase diagram, we now take into account quantum fluctuations in a semiclassical fashion. From the viewpoint of the competition between spin and chirality, it is interesting to develop the continuum descriptions of the two phases—the NAF-dominant phase and the chirality-dominant phase.

A. Low-Energy Fluctuations

In constructing the continuum limit, it is important to find out the relevant low-energy degrees of freedom. To this end, let us calculate the low-energy spectrum in the semiclassical approximation. First we parametrize the semi-classical configuration as:

$$\mathbf{A}_r^{(0)} = (0, 0, (-1)^r \rho_0), \quad \mathbf{B}_r^{(0)} = (0, 0, 0) \quad (39a)$$

for $-\tan^{-1}(1/4) \leq \theta < \theta_{sd} = 0.1476\pi$

or

$$\mathbf{A}_r^{(0)} = (0, 0, 0), \quad \mathbf{B}_r^{(0)} = (0, 0, (-1)^r \rho_0) \quad (39b)$$

for $\theta_{\text{sd}} < \theta < \pi/2$,

where $\rho_0 \equiv \sqrt{n_B}$ ($0 \leq \rho_0 \leq 1$) and is given by (see Appendix A 2):

$$\rho_0 = \begin{cases} \frac{1}{2} \sqrt{\frac{J+4K_4}{J+2K_4}} & \text{for } K_4 < J/2 \\ \frac{1}{4} \sqrt{\frac{-J+8K_4}{K_4}} & \text{for } K_4 > J/2. \end{cases} \quad (40)$$

The value of ρ_0 is plotted in the left panel of Fig. 3.

Now that we have determined the classical (or mean-field) ground state, we are at the point of calculating the spectrum of the low-energy excitations. Let us consider the following small deviation $\delta\mathbf{A}$, $\delta\mathbf{B}$ from the classical ground state:

$$\mathbf{A}_r = \mathbf{A}_r^{(0)} + \delta\mathbf{A}_r, \quad \mathbf{B}_r = \mathbf{B}_r^{(0)} + \delta\mathbf{B}_r. \quad (41)$$

If we plug the above expressions into the classical equation of motion and retain terms up to 1st-order in $\delta\mathbf{A}$ and $\delta\mathbf{B}$, we obtain the following ‘spin-wave’ spectra:

$$\omega_x(k) = \omega_y(k) = \frac{J \cos\left(\frac{k}{2}\right) \sqrt{(3J+4K_4)(3J+4K_4-J\cos(k))}}{\sqrt{2}(J+2K_4)} \quad (42a)$$

$$\omega_z(k) = \sqrt{\frac{\cos(k)J^3 + 4(J+2K_4)J^2 + 2K_4(J^2 - 8K_4J - 16K_4^2)\cos^2(k)}{J+2K_4}}. \quad (42b)$$

It is easy to verify that the transverse modes ($\omega_{x,y}(k)$) have a linear dispersion near the zone boundary $k = \pi$:

$$\omega_{x,y}(k) \approx \frac{J\sqrt{(J+K_4)(3J+4K_4)}}{\sqrt{2}(J+2K_4)} |k - \pi|, \quad (43)$$

while the longitudinal one (ω_z) is gapped (unless $K_4 = J/2$). These linearly dispersive modes roughly describe transverse fluctuations of the director vectors \mathbf{A} and similar to the usual AF magnons. The spectrum for the B-ordered phase (‘chirality-dominant’ phase), which is realized when $K_4 \gg J$, can be obtained in a similar fashion.

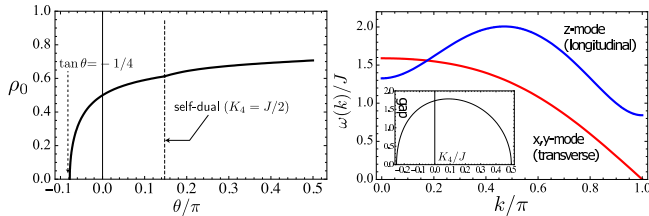


FIG. 3. (color online) (Left): Square-root ρ_0 (Eq. (40)) of the boson density n^B as a function of K_4/J . Note that the boson density ρ_0^2 is always finite. (Right): The low-energy dispersion obtained by a semiclassical (spinwave-like) calculation ($K_4/J = 0.45$). Inset shows the variation of the z -mode gap (at $k = \pi$) as a function of K_4/J . The staggered ordering of \mathbf{A} in the z -direction is assumed. Among the three modes (x , y and z), the longitudinal one (z -direction) may be regarded as the density fluctuation and is massive, while the remaining two are gapless (Goldstone modes) corresponding to the symmetry breaking: $O(3) \rightarrow O(2)$ (In 1D, these Goldstone modes eventually get gapped by strong quantum fluctuations). Only at the self-dual point $K_4/J = 1/2$, the longitudinal branch (z -mode) shows a gapless k -linear behavior.

B. Continuum Limit

The above analysis suggests that we should keep the low-energy order parameter field around $k = \pi$ in constructing the continuum limit for the dominant-NAF phase. Specifically, we use the following *two-sublattice* (plaquette-wise, actually) ansatz to parametrize the \mathbf{A} and \mathbf{B} fields:

$$\mathbf{A}_r + i\mathbf{B}_r = \sqrt{\rho_0^2 + a l_\phi(x)} (-1)^r \mathbf{e}^{i\phi(x)} \times \left\{ \sqrt{1 - a^2 \mathbf{l}_\Omega^2(x)} \mathbf{\Omega}(x) + ia(\mathbf{\Omega} \times \mathbf{l}_\Omega) \right\}, \quad (44)$$

where the order parameter field (*director*) satisfies $|\mathbf{\Omega}(x)| = 1$ and $\mathbf{\Omega} \cdot \mathbf{l}_\Omega = 0$. Physically, the two small fields \mathbf{l}_Ω and l_ϕ are respectively the generators of spin-SU(2) and charge-U(1):

$$\begin{aligned} \mathbf{T}_r^\alpha &= -i\epsilon_{\alpha\beta\gamma} b_\beta^\dagger b_\gamma = 2\rho_0^2 a (\mathbf{l}_\Omega)^\alpha + \dots \\ n_B &= \sum_\alpha b_\alpha^\dagger b_\alpha = \rho_0^2 + a l_\phi(x) + \dots \end{aligned} \quad (45)$$

The vector order parameter $\mathbf{\Omega}$ represents spin and chirality in a unifying manner. When the phase ϕ is dominantly around $\phi = 0$ or π , the order parameter $\mathbf{\Omega}$ describes the transverse fluctuations of the (π, π) antiferromagnetic order represented by \mathbf{A} :

$$\mathbf{\Omega} \sim (\mathbf{S}_1 - \mathbf{S}_2)_{q=\pi}. \quad (46)$$

When ϕ fluctuates around $\pm\pi/2$, on the other hand, $\mathbf{\Omega}$ constitutes the imaginary part of the quantity $\mathbf{A} + i\mathbf{B}$ and describes the fluctuations of (the staggered component of) the vector chirality \mathbf{B} :

$$\mathbf{\Omega} \sim (\mathbf{S}_1 \times \mathbf{S}_2)_{q=\pi}. \quad (47)$$

As in the usual Haldane mapping⁴⁵, in order to write down the effective action, we assume that the two fields \mathbf{l}_Ω and l_ϕ are small compared with Ω and retain terms up to second-order in the calculation. The condensate amplitude ρ_0 and the phase angle ϕ_0 of the ground state can be determined by minimizing the constant part of the effective action:

$$E_0 = \rho_0^2 \{ \rho_0^2 (J + 6K_4) - 6K_4 \} - \rho_0^2 (1 - \rho_0^2) (J - 2K_4) \cos(2\phi_0). \quad (48)$$

Depending on the sign of $(J - 2K_4)$, either $\phi_0 = 0, \pi$ or $\phi_0 = \pi/2, 3\pi/2$ is chosen.

After some algebra, we obtain (see Appendix A 2 for details):

$$\begin{aligned} \mathcal{S}_{\text{eff}}[\Omega] = & \frac{1}{2} \chi_s \int dx dt (\partial_t \Omega)^2 - \frac{1}{2} \rho_s \int dx dt (\partial_x \Omega)^2 \\ & + \frac{1}{2} \chi_c \int dx dt (\partial_t \phi)^2 - \frac{1}{2} \rho_c \int dx dt (\partial_x \phi)^2 \\ & + g(J, K_4) \int dx dt \cos(2\phi(x, t)), \end{aligned} \quad (49)$$

where the explicit expressions for the five coupling constants (spin/charge susceptibility $\chi_{s/c}$, the spin/charge stiffness $\rho_{s/c}$ and the sine-Gordon coupling $g(J, K_4)$) are given in Appendix (Eq. (A13)). Note that a similar effective action (without the cosine-term) has been derived in the context of $F = 1$ spinor Bose-Einstein condensate.^{49,50}

The spin part of the effective action is nothing but the $O(3)$ non-linear sigma model in $(1+1)$ -dimensions, where the long-range-ordered ground state with the gapless k -linear Goldstone modes is replaced by a quantum-disordered one with the gapped triplet excitations (*triplon*).⁵¹ Since near $\theta = 0$ and π , Ω may be thought of as the order parameter for the standard (π, π) AF ordering, the spin part describes the short-range antiferromagnetic fluctuations for $J > K_4$. Since \mathbf{A} and \mathbf{B} play the role of the director in the spin-nematic, one may think that the order parameter manifold is \mathbb{RP}^2 . However, in contrast to the case of the usual spin nematic, the directors (\mathbf{A} and \mathbf{B}) themselves are directly related to the physical observables (i.e. $\mathbf{S}_1 - \mathbf{S}_2$ and $\mathbf{S}_1 \times \mathbf{S}_2$, respectively) and the order parameter in fact is defined on the two-dimensional sphere S^2 . In principle, there can be a topological term associated with $\Pi_2(S^2)$ in the above effective action. However, the above direct mapping suggests that there is no such topological term in the effective action.

On top of the spin part, there is the spin-chirality (or, in terms of spin-1 bosons, ‘charge’) part which describes the dynamics of the Bose phase ϕ ; the spin-chirality part of the effective action is given by the sine-Gordon model with the (J, K_4) -dependent couplings. Depending on the sign of $g(J, K_4)$, the cosine term pins the ground-state phase either at $\phi = 0, \pi$ (for $g(J, K_4) > 0$) or at $\phi = \pi/2, 3\pi/2$ (for $g(J, K_4) < 0$). Since $\phi \mapsto \phi + \pi$ amounts to the 1-site translation $r \mapsto r + 1$ (see Eq. (44)), one can see that in both cases there appear two-fold degenerate ground states related by 1-site translation; the sine-Gordon soliton connects the two degenerate ground states. At the self-dual point $K_4 = J/2$, the

sine-Gordon coupling disappears and the charge (i.e. spin-chirality) part reduces to the Tomonaga-Luttinger model as is expected from the previous results.^{35,36}

Now we proceed to a more interesting case of the chirality-dominant phase realized in the large- K_4 region. In this phase, ϕ_0 is locked at $\phi = \pm\pi/2$ and the effective action (49) describes the short-range (staggered) fluctuations in the chirality channel; the staggered component of the \mathbf{B} -field plays a role of the order-parameter field: $\Omega \sim (\mathbf{S}_1 \times \mathbf{S}_2)_{q=\pi}$. As before, the ground state is quantum-disordered with a gapped triplet excitation, which is created not by the spin operators themselves but by the staggered component of the vector chirality $(\mathbf{S}_1 \times \mathbf{S}_2)_{q=\pi}$. This agrees with the results of numerical simulations.^{27,28} Since the duality transformation ($\varphi = \pi/2$ in Eq. (22) or $\phi \mapsto \phi + \pi/2$ in Eq. (44)) interchanges two vector fields \mathbf{A} (‘spin’) and \mathbf{B} (‘chirality’), these two effective action (49) clearly exhibit the ‘dual’ nature of spin and chirality in the model (1).

To summarize, we have obtained the $O(3)$ non-linear sigma model for the spin dynamics in the NAF/chirality-dominant phases; deep inside these phases, where the spin-chirality (θ) fluctuations have a large gap and are well separated from the transverse spin fluctuations (see the inset of Fig. 3), we may expect that the *pure* sigma model provides us with a good description of the low-energy physics far away from the self-dual point $K_4/J = 1/2$. Since a similar non-linear sigma model is obtained in the standard field-theory treatment⁵² of the two-leg ladder with $K_4 = 0$, one may identify the NAF-dominant phase with the rung-singlet (RS) phase. However, as we will see below, this is not the case. It is important to note that the above derivation of the effective action applies to higher dimensional cases as well with due modification of their coupling constants $\rho_{s,c}$ and $\chi_{s,c}$.

When the self-dual point $K_4/J = 1/2$ is approached, on the other hand, the gap of the ω_z -branch (i.e. the ϕ -channel) decreases and eventually becomes smaller than the dynamically-generated spin gap; exactly at the point, the longitudinal mode exhibits the gapless k -linear behavior⁵³ around $k = \pi$ which we may identify with the gapless spin-chirality (i.e. the $U(1)$ -phase of the spin-1 hardcore boson) fluctuations represented by the Tomonaga-Luttinger model also found in the bosonization analysis.^{35,36} As the gap in the spin sector (which is described by the non-linear sigma model) is always finite, the quantum phase transition between NAF-dominant phase and the chirality-dominant one is described by the $c = 1$ Tomonaga-Luttinger liquid.³⁶ In fact, around the self-dual point, the spin-singlet phase (‘charge’) fluctuations play the primary role.

Away from the self-dual point, the anomalous hopping term generates the $\cos 2\phi$ -term which pins the ground state at $\phi = 0, \pi$ or at $\phi = \pi/2, 3\pi/2$ to stabilize the two-fold degenerate ground states of the model (1) as far as the condensate amplitude ρ_0 is finite; the two-fold degeneracy corresponds to breaking of the \mathbb{Z}_2 -symmetry $(\mathbf{A}, \mathbf{B}) \mapsto (-\mathbf{A}, -\mathbf{B})$ (i.e. the interchange of the two chains $1 \leftrightarrow 2$) or the 1-site translation $r \mapsto r + 1$. In 1D, the rotation symmetry is restored and the only broken symmetry is the \mathbb{Z}_2 . This is what we have in the staggered-dimer phase and the staggered-scalar-chirality

phase.²⁷ In the case of the two-leg ladder, the spin excitations are always the gapped triplons in the three main phases (*singlet-product*, *NAF/chirality-dominant*) in the $J > 0$ region (see Fig. 2) and only the presence/absence of the \mathbb{Z}_2 -symmetry distinguishes between the first- and the latter two phases. In this respect, the NAF-dominant- and the chirality-dominant phase may be identified respectively with the staggered dimer phase and the staggered scalar chiral phase found in Ref. 27. Since our semiclassical treatment underestimates the effect of quantum fluctuations brought about by the pairing term, the \mathbb{Z}_2 -broken ordered states (NAF/chirality-dominant phases) are more stabilized than in the actual two-leg ladder.²⁷

Last, we briefly touch upon the effective action in the F-nematic phase. A similar fluctuation analysis shows that the gapless k -linear modes appear at $k = 0$ in this case. The calculation is essentially the same as in the previous two cases except that we adopt the following parametrization reflecting the gapless transverse modes at $k = 0$:

$$\begin{aligned} \mathbf{A}_r + i \mathbf{B}_r &= \sqrt{\rho_0^2 + a l_\phi(x)} e^{(-1)^r i \phi(x)} \\ &\times \left\{ \sqrt{1 - a^2 \mathbf{l}_\Omega^2(x)} \mathbf{\Omega}(x) + i a (\mathbf{\Omega} \times \mathbf{l}_\Omega) \right\}. \end{aligned} \quad (50)$$

The staggered definition of the Bose phase $e^{(-1)^r i \phi(x)}$ has been inspired by the gapless k -linear mode appearing at the point $J + 2K_4 = 0$ reflecting the existence of an alternating spin-chirality $U(1)$ -symmetry.⁵⁴ As in the above cases, we carry out gradient expansion and the subsequent Gaussian integration over $\mathbf{l}_\Omega, l_\phi$ to obtain the non-linear sigma model (49) with different coupling constants (see Eq. (A16)). At the transition point ($J + 2K_4 = 0$) between partial-AF and F-nematic, the sine-Gordon interaction vanishes and the transition is described by the Tomonaga-Luttinger liquid. Again, quantum fluctuations open a gap in the spin sector and the ground state is characterized by the short-range correlation of the collinear order parameter $\mathbf{\Omega} \sim \mathbf{S}_1 - \mathbf{S}_2$ at $k = 0$, which is consistent with the numerical observation.²⁷

V. EFFECTS OF MAGNETIC FIELD AND MUTUAL INDUCTION PHENOMENA

In this section, we investigate the effect of a magnetic field on the two-leg spin ladder with a ring-exchange by means of our semiclassical approach. We show, as a by-product, that the spin-chirality duality leads to an interesting phenomenon—*mutual induction between spin and chirality* degrees of freedom.

To this end, it is convenient to enlarge the parameter space of model (1) and consider a two-leg ladder with a general four-spin exchange interaction:³⁶

$$\mathcal{H} = g_1 \mathcal{H}_1 + g_2 \mathcal{H}_2 + g_3 \mathcal{H}_3 + g_4 \mathcal{H}_4 + g_5 \mathcal{H}_5 + g_6 \mathcal{H}_6, \quad (51)$$

where the six building blocks are given as:³⁶

$$\mathcal{H}_1 = \sum_r (\mathbf{S}_{1,r} + \mathbf{S}_{2,r}) \cdot (\mathbf{S}_{1,r+1} + \mathbf{S}_{2,r+1}) \quad (52a)$$

$$\mathcal{H}_2 = \sum_r (\mathbf{S}_{1,r} - \mathbf{S}_{2,r}) \cdot (\mathbf{S}_{1,r+1} - \mathbf{S}_{2,r+1}) \quad (52b)$$

$$\begin{aligned} \mathcal{H}_3 &= 4 \sum_r [(\mathbf{S}_{1,r} \cdot \mathbf{S}_{1,r+1})(\mathbf{S}_{2,r} \cdot \mathbf{S}_{2,r+1}) \\ &\quad + (\mathbf{S}_{1,r} \cdot \mathbf{S}_{2,r+1})(\mathbf{S}_{2,r} \cdot \mathbf{S}_{1,r+1})] \end{aligned} \quad (52c)$$

$$\mathcal{H}_4 = 4 \sum_r (\mathbf{S}_{1,r} \times \mathbf{S}_{2,r}) \cdot (\mathbf{S}_{1,r+1} \times \mathbf{S}_{2,r+1}) \quad (52d)$$

$$\mathcal{H}_5 = \frac{1}{2} \sum_r (\mathbf{S}_{1,r} \cdot \mathbf{S}_{2,r} + \mathbf{S}_{1,r+1} \cdot \mathbf{S}_{2,r+1}) \quad (52e)$$

$$\mathcal{H}_6 = \sum_r (\mathbf{S}_{1,r} \cdot \mathbf{S}_{2,r})(\mathbf{S}_{1,r+1} \cdot \mathbf{S}_{2,r+1}). \quad (52f)$$

The six coupling constants are expressed in terms of the six bosonic ones as:

$$\begin{aligned} g_1 &= J_{bl} - J_{bq}/2, \quad g_2 = (t + u)/2, \quad g_3 = J_{bq}/2, \\ g_4 &= (t - u)/2, \quad g_5 = 2J_{bq} - \mu + 3V_c/2, \quad g_6 = V_c. \end{aligned} \quad (53)$$

Under the spin-chirality duality symmetry (2), the coupling constants of model (51) transform as: $g_2 \leftrightarrow g_4$, while all the others remain invariant.

A. Mean-field analysis

Let us consider the situation where the magnetic interaction J_{bl} of model (11) (i.e. g_1 in the ladder model (51)) is dominant and the interaction $g_2 (> 0)$ in the spin-spin channel is stronger than that in the chirality channel g_4 . The idea is as follows. When a sufficiently strong magnetic field (say, in the z -direction) induces uniform magnetization, the magnetic moments $\mathbf{M} = \mathbf{S}_1 + \mathbf{S}_2 = -2\mathbf{A} \times \mathbf{B}$ (see Eq. (23)) assume (at least in the semiclassical sense) the *canted* configuration as is shown in Fig. 4. A simple mean-field argument given above concludes that the anti-parallel ordering of $\mathbf{A} \propto \mathbf{S}_1 - \mathbf{S}_2$ forces the canting of the chirality vector $\mathbf{B} \propto \mathbf{S}_1 \times \mathbf{S}_2$ leading to the appearance of finite vector chirality in the field direction:⁵⁵ $(\mathbf{S}_1 \times \mathbf{S}_2)^z \neq 0$ (see Fig. 4). Note that the mean-field (or variational) energy is invariant under the *global* \mathbb{Z}_2 -symmetry: $\mathbf{A} \mapsto -\mathbf{A}, \mathbf{B} \mapsto -\mathbf{B}$ corresponding to the interchange of the two chains $1 \leftrightarrow 2$. Therefore, the appearance of uniform vector chirality in the low-field phase is accompanied by the \mathbb{Z}_2 -symmetry breaking.

According to the spin-chirality duality (2), the same argument applies to the case where the chirality channel $g_4 (> 0)$ is dominant; in this case, the ordering in the chirality channel induces finite $(\mathbf{S}_1 - \mathbf{S}_2)^z$, that is, magnetization is induced *asymmetrically* in the upper- and the lower chain. It is important to note that, when the interaction in the spin-spin channel

is dominant, the chirality is induced and vice versa. As is clear from the above argument, this is not restricted to one dimension; our semiclassical approach immediately predicts that in two dimensions too. One of the most important conclusions of our bosonic effective theory is that this *mutual induction* is an observable consequence of the spin-chirality duality.

It would be interesting to check if the simplest ring-exchange ladder (1) really supports this phase or not. Again we can use mean-field analysis to map out the phase diagram in the presence of magnetic field. The result is summarized in Fig. 5. Except for the trivial saturated phase which covers the entire ferromagnetic phase as well as the high-field region, the 1/2-plateau phase, which is characterized by spin-polarized spin-1 bosons sitting every other site, occupies the large portion of the phase diagram. This is consistent with the previous results obtained by numerical simulations and strong-coupling expansions.^{54,56}

Magnetization increases smoothly in the two collinear phases (*collinear-I* and *collinear-II*). In the collinear-I phase, both **A** and **B** align in an AF manner and are perpendicular to the field (hence the local moments $\propto \mathbf{A} \times \mathbf{B}$ are parallel to the field. See Fig. 6(a)). It exists typically in the low-field region of ‘NAF-dominant’ phase and in the high-field region near saturation. In fact, it is easy to show, by finding the exact single-magnon wave function, that it is a generalizations of (the simplest version of) the triplon condensate at momentum $k = \pi$ which is used frequently in analyzing the magnetization process of dimer systems; here not only the spin component parallel (i.e. $T^z = +1$) to the field but also the anti-parallel (i.e. $T^z = -1$) one are taken into account.⁵⁷ The collinear-II phase (Fig. 6(b)) is similar to the collinear-I except that here both **A** and **B** align ferromagnetically. In this sense, this is thought of as the classical counterpart of the triplon condensate at $k = 0$. Typically, it appears when the field is applied in the ‘F-nematic’ phase.

On top of them, yet another collinear phase (dubbed *SDW* for spin density wave) appears in the ‘partial-AF’ phase when the field is very weak (a tiny region below the 1/2-plateau). In the SDW phase, the local moments $\langle \mathbf{T} \rangle$ form an up-down pattern along the field direction while the lengths of the moments on different sublattices are not equal (Fig. 6(c)).

Our mean-field results basically agree with those of density-matrix-renormalization-group⁵⁸ (DMRG) simulations;⁵⁴ the exceptions are the ‘SDW’ phase and ‘collinear-II’ near saturation. In fact, in the region where we found ‘SDW’, DMRG simulations observed a phase with the dominant vector-chiral correlation (in the transverse direction). As we have remarked above, already at the mean-field level, the energies of ‘chirality-dominant’ phase and ‘SDW’ are very close to each other and the correct treatment of quantum fluctuations might stabilize the chirality over ‘SDW’ state. ‘Collinear-II’ state in the classical limit translates in the quantum description to the *single-boson* (either triplons over the rung singlet or singlet-rungs in the spin-polarized state) condensate at $k = 0$. In the low-field region, this is consistent with the phase diagram (Fig. 1 and 5 of Ref. 54) obtained numerically. However, what has been observed near saturation is the phase characterized by the condensation of

magnon bound states. The failure of our mean-field theory in describing this magnon-pair phase is not surprising since our wave function is tailored to describe the single-boson condensate.

Clearly, the mean-field (θ, H) -phase diagram (Fig. 5) of the ring-exchange ladder (1) shows that the spin-canted state illustrated in Fig. 4 is not realized at least in the simplest ladder. In fact, after this phenomenon of magnetization-induced vector chirality has been predicted first in one dimension by means of bosonization,⁴² extensive DMRG study⁵⁴ has been carried out to show that the pure ring-exchange model (1) in a magnetic field is not sufficient to support the predicted phase with finite uniform (vector) chirality. This is consistent with our mean-field study.

To seek for the possibility of the new phase with uniform chirality, we explored the enlarged parameter space and extensively carried out the variational analysis. It turned out that it is not easy to realize the canted state (Fig. 4) at intermediate fillings (i.e., $0 < n_B < 1$); it is quite often masked by the above three collinear states or the 1/2-plateau. However, careful choices of parameters can stabilize the canted state. For instance, we show the magnetization process of the generalized ladder with $J_{bl} = 2.0$, $J_{bq} = 0.0$, $J_A = (t + u)/2 = 1.3$, $J_B = (t - u)/2 = 0.01$, $V_c = 0.6$, $\mu = -0.5$ in Fig. 7. One can clearly see that uniform z -component of vector chirality is induced in the low-field region. As has been mentioned above, the appearance of uniform vector chirality in the low-field phase implies the breaking of the chain-exchange \mathbb{Z}_2 -symmetry.

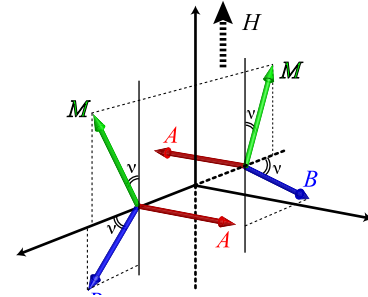


FIG. 4. (color online) A naively expected high-field configuration of $\mathbf{A} \propto \mathbf{S}_1 - \mathbf{S}_2$, $\mathbf{B} \propto \mathbf{S}_1 \times \mathbf{S}_2$, and $\langle \mathbf{T} \rangle \propto \mathbf{S}_1 + \mathbf{S}_2$. Spin (**T**) canting induces a *uniform* z -component $(\mathbf{S}_1 \times \mathbf{S}_2)^z$. If a similar spin-canted state is realized for large enough g_4 , we may expect a state where local magnetization is induced asymmetrically in the two chains $\langle S_1^z \rangle \neq \langle S_2^z \rangle$.

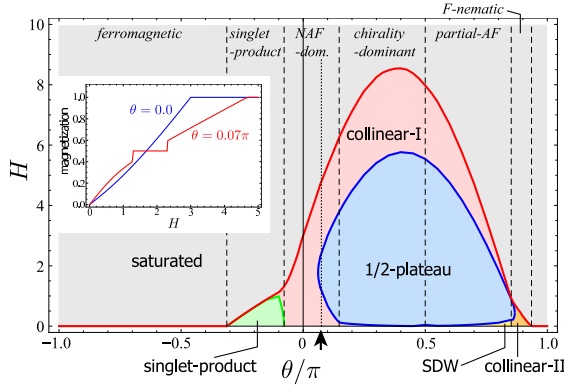


FIG. 5. (color online) Mean-field phase diagram of the ring-exchange ladder in magnetic field ($J = \cos \theta$, $K_4 = \sin \theta$). The large portion of the parameter space is occupied by 1/2-plateau phase. All the phases except the singlet-product phase are *collinear* and are characterized by parallel or anti-parallel alignment of \mathbf{A} , \mathbf{B} and $\langle \hat{\mathbf{T}} \rangle$. The canted phase anticipated in the text does *not* appear in this parameter space. Inset: magnetization curves for $\theta = 0$ and 0.07π (marked by an arrow head in the main panel).

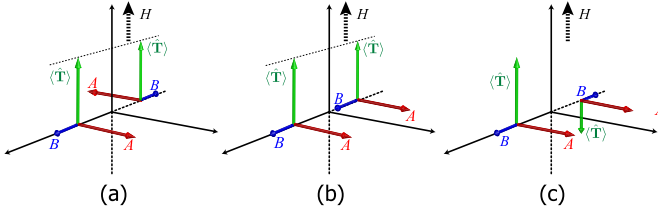


FIG. 6. (color online) Three collinear configurations exhibiting smooth magnetization process: (a) ‘collinear-I’, (b) ‘collinear-II’ and (c) ‘SDW’. The configuration (a) generically appears in the high-field region, while (b) realizes when the field is applied in the ‘F-nematic’ phase (see Fig. 5). In the configurations (a) and (b), z -component of local magnetization T^z and local boson density n_B are uniform. In the (c) configuration, on the other hand, these quantities alternate along the ladder to form a density-wave state.

B. Numerical results

In order to investigate the possible appearance of vector chirality, we now turn to numerical investigation using the DMRG algorithm.⁵⁸ Since the pure ring-exchange model does not exhibit such a symmetry breaking,⁵⁴ and because the most general spin ladder Hamiltonian contains too many parameters, we have used the previous variational analysis as a guide.

Using the following parameters $J_{bl} = 2.0$, $J_{bq} = 0.0$, $(t - u)/2 = 0.01$, $V_c = 0.6$, and $\mu = -0.5$, vector chirality was found to occur for $(t + u)/2 = 1.2$ in the variational approach (see Fig. 7). In Fig. 8, we plot the vector chirality correlation

$$C(x) = \langle (\mathbf{S}_{1,r} \times \mathbf{S}_{2,r})^z (\mathbf{S}_{1,r+x} \times \mathbf{S}_{2,r+x})^z \rangle \quad (54)$$

obtained numerically with DMRG. We have studied $2 \times L$

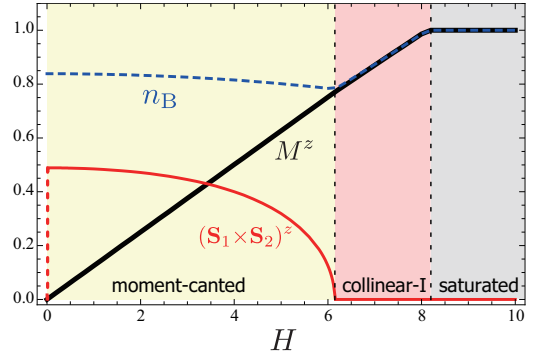


FIG. 7. (color online) Magnetization process exhibiting the anticipated canted configuration: $J_{bl} = 2.0$, $J_{bq} = 0.0$, $(t + u)/2 = 1.2$, $(t - u)/2 = 0.01$, $V_c = 0.6$, $\mu = -0.5$. At around $H = 6.2$, spin state changes from the canted state to the collinear-I (with a kink in n_B). The vector chirality $(\mathbf{S}_1 \times \mathbf{S}_2)^z$ is finite in small-field region where the local magnetization assumes canted configuration (‘moment-canted’).

ladders with general four-spin exchange (see Eq. (51)) corresponding to the above bosonic parameters, and we use open boundary conditions. Correlations are averaged with $L/4 \leq r \leq 3L/4$. We keep up to 1200 states which is sufficient to get a discarded weight smaller than 10^{-12} .

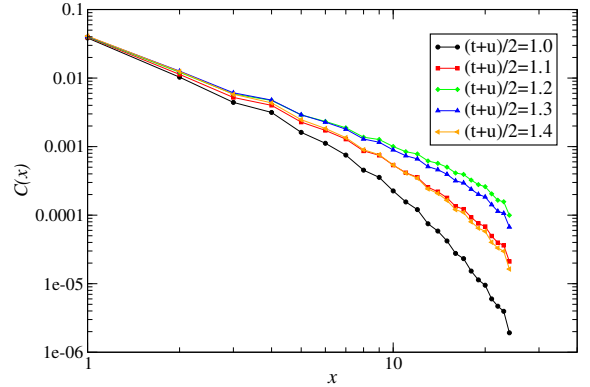


FIG. 8. (color online) Vector chirality correlations obtained on 2×32 ladder with parameters given in the text. Magnetization was fixed at 1/4 of its saturation value.

As can be read from the plot, vector chirality correlations do exhibit a slight increase when $(t + u)/2 \sim 1.2$, corresponding to the optimal parameter found in the variational analysis, but this only indicates quasi long-range order, i.e. an algebraic decay.

We have also tried to vary some of these parameters, or look at other magnetization values, but we have been unable so far to detect any evidence of long-range order.

VI. CONCLUDING REMARKS

In the present paper, we have investigated the phase diagram of the two-leg spin ladder with a ring-exchange interaction. In this respect, we have developed a unifying approach which treats AF fluctuations and VC (or p -nematic) ones on the same footing. This approach is based on the description in terms of a spin-1 hardcore boson operators that create the triplet states out of the singlet on each rung. The spin-chirality transformation, originally defined on the lattice spin operators,^{28,29} has a simple physical meaning here through the standard $U(1)$ global gauge symmetry of the bosons.

Using a simple mean-field calculation on the boson operators, we have mapped out the zero-temperature phase diagram of the two-leg spin ladder with a ring-exchange interaction. This bosonic approach enables one to take into account quantum fluctuations in a semiclassical fashion. In particular, we reproduce the main results of previous intensive numerical studies^{27,28} and a low-energy description of the chirality-dominant phase is derived within the semiclassical analysis.

The effect of a magnetic field can also be naturally analyzed in our bosonic approach. We reveal the mutual induction phenomenon between spin and chirality degrees of freedom with the emergence of a vector-chirality phase, e.g. with long-range ordering $(\mathbf{S}_1 \times \mathbf{S}_2)^z \neq 0$, by the application of a strong magnetic field along the z -axis. Within a mean-field approach, we found that the two-leg spin ladder with a ring-exchange interaction (Eq. (1)) in a magnetic field does not support this exotic phase in full agreement with the DMRG study of Ref. 54. In this respect, we have given conditions to observe this phase by considering a two-leg spin ladder with general four-spin exchange interactions. Unfortunately, our preliminary DMRG results could not find any evidence of chirality long-range ordering, although a mean-field analysis predicts a finite window where uniform vector chirality along the magnetic field is stabilized. Clearly extensive large-scale DMRG calculations are called for to fully investigate the six-parameters space of the problem and look for the existence of the magnetic-field induced vector-chirality phase.

Finally, we briefly comment on a perspective. As we have mentioned above, our bosonic approach can be readily generalized to higher-dimensional systems made of two-spin clusters (spin dimers) like $S = 1/2$ bilayer systems. However, the range of its applicability is much broader. In fact, as we will show elsewhere,⁴⁸ even in the two-dimensional cases *without* such special structures, one can construct effective bosonic degrees of freedom which encode the competition between spin and chirality degrees of freedom in close parallel to the 1D case. Then, we can apply a semiclassical field-theory approach similar to what is described in this paper to such higher-dimensional systems as the spin-1/2 Heisenberg model on the square lattice with a ring-exchange interaction to capture the global structure of the phase diagram.

ACKNOWLEDGEMENTS

The authors thank F. Essler, T. Hikihara, A. Kolezhuk, A. Läuchli, C. Lhuillier, F. Mila, M. Oshikawa, and M. Sato for helpful discussions. We also wish to thank the organizers of the workshop/symposium *Yukawa International Seminar (YKIS) 2007* and *Topological Aspects of Solid State Physics* held at Yukawa Institute for Theoretical Physics where parts of this work were carried out. One of the authors (KT) is grateful to Max-Planck Institute for the physics of complex systems, where this work was completed, for the hospitality. The author (KT) was supported in part by Grant-in-Aids for Scientific Research (C) 18540372, (C) 20540375, and Priority Areas “Novel States of Matter Induced by Frustration” (No.19052003) from MEXT, Japan and by the global COE (GCOE) program ‘The next generation of physics, spun from universality and emergence’ of Kyoto University. One of the authors (SC) would like to thank Institut Universitaire de France for financial support.

Appendix A: Dimer coherent state path integral

In this Appendix, we present some technical details on the derivation of the low-energy effective actions for the RS and VC phases of the two-leg spin ladder with a ring-exchange (1).

1. Berry phase term

The quantum dynamics is generated by the Berry phase term which can be derived from the following overlap:

$$\langle s(t + \delta t), \mathbf{t}(t + \delta t) | s(t), \mathbf{t}(t) \rangle \approx 1 + \{ s \partial_t s^* + \mathbf{t} \cdot \partial_t \mathbf{t}^* \} \delta t, \quad (\text{A1})$$

where t and $t + \delta t$ denote two infinitesimally separated times. Plugging (19) into the above, we obtain

$$\begin{aligned} \langle s(t + \delta t), \mathbf{t}(t + \delta t) | s(t), \mathbf{t}(t) \rangle &= 1 + i(\mathbf{A} \cdot \partial_t \mathbf{B} - \mathbf{B} \cdot \partial_t \mathbf{A}) \delta t \\ &= 1 - \frac{1}{2}(\mathbf{t}^* \cdot \partial_t \mathbf{t} - \mathbf{t} \cdot \partial_t \mathbf{t}^*) \delta t, \quad (\text{A2}) \end{aligned}$$

from which we can read off the Berry phase contribution to the (single-site) action:

$$S_{\text{Berry}} = \int dt \frac{i}{2}(\mathbf{t}^* \cdot \partial_t \mathbf{t} - \mathbf{t} \cdot \partial_t \mathbf{t}^*) = \int dt (\mathbf{A} \cdot \partial_t \mathbf{B} - \mathbf{B} \cdot \partial_t \mathbf{A}). \quad (\text{A3})$$

This Berry phase term is the first contribution of the general action (26). As is easily seen by rescaling: $\mathbf{t} \mapsto \sqrt{\rho} \mathbf{t}$ ($|\mathbf{t}| = 1$), this term generates the dynamics in the *transverse* direction, i.e. there is no time-derivative for the ρ -field which describe the fluctuations in the *longitudinal* direction.

2. Continuum limit

On the basis of the fluctuation analysis in Sec. IV A, we can derive a low-energy effective actions for the NAF-dominant- and the chirality-dominant phase. Since the \mathbf{A} -field develops in the former phase, we may make the following ansatz Eq. (44) to parametrize the \mathbf{A} and \mathbf{B} fields:

$$\begin{aligned} \mathbf{A}_r + i\mathbf{B}_r &= \sqrt{\rho_0^2 + a l_\phi(x)} (-1)^r \mathbf{e}^{i\phi(x)} \\ &\times \left\{ \sqrt{1 - a^2 \mathbf{l}_\Omega^2(x)} \mathbf{\Omega}(x) + ia(\mathbf{\Omega} \times \mathbf{l}_\Omega) \right\}. \end{aligned} \quad (\text{A4})$$

Clearly, $\mathbf{\Omega}$ and ϕ respectively describe the transverse- and the phase fluctuations of the spin-1 boson. To guarantee the normalization condition $\langle n_B \rangle = \rho_0^2$, we impose the following constraints:

$$|\mathbf{\Omega}| = 1, \quad \mathbf{\Omega} \cdot \mathbf{l}_\Omega = 0. \quad (\text{A5})$$

The idea underlying the decomposition (A4) may be seen as follows. First we note that Eq. (A4) is a close parallel of the expression (27). Suppose that the vector field \mathbf{A} has a finite length ρ_0^2 (as in NAF-dominant phase) and that it plays a role of the order parameter i.e. $\mathbf{\Omega} \sim \mathbf{A}$. The imaginary part \mathbf{B} may be obtained by noting that the SU(2)-generator is given by

$$\mathbf{L}_r = -2\mathbf{A}_r \times \mathbf{B}_r \quad (\text{A6})$$

(see Eq. (23)). As is suggested by counting the number of independent degrees of freedom, once the overall phase ϕ is singled out, the angle between \mathbf{A}_r and \mathbf{B}_r cannot be arbitrary; a convenient choice would be to take: $\mathbf{A}_r \cdot \mathbf{B}_r = 0$. When $\mathbf{A}_r \sim \mathbf{\Omega}_r$, \mathbf{B}_r is expressed simply as:

$$\mathbf{\Omega}_r \times \mathbf{L}_r = -2 \{ (\mathbf{\Omega}_r \cdot \mathbf{B}_r) \mathbf{\Omega}_r - (\mathbf{\Omega}_r)^2 \mathbf{B}_r \} = 2\mathbf{B}_r \quad (\perp \mathbf{A}_r). \quad (\text{A7})$$

With the identification: $\mathbf{l}_\Omega \sim \mathbf{L}/2$, one can see that the vectorial part of (A4) correctly reproduces the transformation properties of $\mathbf{A} + i\mathbf{B}$. The phase part $\sqrt{\rho_0^2 + a l_\phi(x)} \mathbf{e}^{i\phi(x)}$ is easily guessed from the well-known result in the single-component Bose liquid⁵⁹.

Now let us plug the ansatz (A4) into the action (26) and keep terms up to second order in the small fields \mathbf{l}_Ω and l_ϕ . The constant part (49)

$$E_0 = \rho_0^2 \{ \rho_0^2 (J + 6K_4) - 6K_4 \} - \rho_0^2 (1 - \rho_0^2) (J - 2K_4) \cos(2\phi_0) \quad (\text{A8})$$

is minimized to give ρ_0 and ϕ_0 :

$$\begin{aligned} (\rho_0, \phi_0) &= \begin{cases} \left(\frac{1}{2} \sqrt{\frac{J+4K_4}{J+2K_4}}, 0 \text{ (or } \pi) \right) & \text{for } -1/4 < K_4/J < 1/2 \\ \left(\frac{1}{4} \sqrt{\frac{-J+8K_4}{K_4}}, \frac{\pi}{2} \text{ (or } \frac{3\pi}{2}) \right) & \text{for } K_4/J > 1/2. \end{cases} \end{aligned} \quad (\text{A9})$$

Dropping the alternating sums and changing the sum over rungs to integrals

$$\sum_r \mapsto \frac{1}{a} \int dx, \quad (\text{A10})$$

we obtain the following results:⁶⁰

$$\mathcal{S}_{\text{Berry}} = \int dx dt \left\{ l_\phi (\partial_t \phi) + 2\rho_0^2 \mathbf{l}_\Omega \cdot [\mathbf{\Omega} \times (\partial_t \mathbf{\Omega})] + \frac{\rho_0^2}{a} (\partial_t \phi) \right\}, \quad (\text{A11a})$$

$$\begin{aligned} \mathcal{S}_{\text{magnetic}} + \mathcal{S}_{\text{charge}} &\approx - (2J + 4K_4) \rho_0^4 a \int dx dt (\mathbf{l}_\Omega)^2 - 4K_4 a \int dx dt l_\phi^2, \end{aligned} \quad (\text{A11b})$$

and

$$\begin{aligned} \mathcal{S}_{\text{hopping}} &\approx - \left\{ \left(\frac{J}{2} + K_4 \right) \pm \left(\frac{J}{2} - K_4 \right) \right\} a \\ &\times \rho_0^2 (1 - \rho_0^2) \int dx dt \left\{ [(\partial_x \mathbf{\Omega})^2 + (\partial_x \phi)^2] + 2l_\phi^2 \right\} \\ &\mp 4a \rho_0^2 (1 - \rho_0^2) \left(\frac{J}{2} - K_4 \right) \int dx dt (\mathbf{l}_\Omega)^2, \end{aligned} \quad (\text{A11c})$$

where the upper (lower) sign is chosen when $J > 2K_4$ ($J < 2K_4$). The Gaussian integration in \mathbf{l}_Ω and l_ϕ yields the following result:

$$\begin{aligned} \mathcal{S}_{\text{eff}}[\mathbf{\Omega}] &= \frac{1}{2} \chi_s \int dx dt (\partial_t \mathbf{\Omega})^2 - \frac{1}{2} \rho_s \int dx dt (\partial_x \mathbf{\Omega})^2 \\ &+ \frac{1}{2} \chi_c \int dx dt (\partial_t \phi)^2 - \frac{1}{2} \rho_c \int dx dt (\partial_x \phi)^2 \\ &+ g(J, K_4) \int dx dt \cos(2\phi). \end{aligned} \quad (\text{A12})$$

When $J > 2K_4$, the effective action $\mathcal{S}_{\text{eff}}[\mathbf{\Omega}]$ describes the (π, π) AF fluctuations and the phase fluctuations in the spin-chirality space. The five coupling constants $\chi_{s,c}$, $\rho_{s,c}$ and $g(J, K_4)$ are given by:

$$\chi_s = \frac{J + 4K_4}{4aJ(J + K_4)}, \quad \rho_s = \frac{J(J + 4K_4)(3J + 4K_4)a}{8(J + 2K_4)^2}, \quad (\text{A13a})$$

$$\chi_c = \frac{1}{4a(J + 2K_4)}, \quad \rho_c = \frac{J(J + 4K_4)(3J + 4K_4)a}{8(J + 2K_4)^2}, \quad (\text{A13b})$$

$$g(J, K_4) = \frac{(J - 2K_4)(J + 4K_4)(3J + 4K_4)}{16(J + 2K_4)^2 a} (> 0). \quad (\text{A13c})$$

Note that precisely at the self-dual point $J = 2K_4$, $g(J, K_4) = 0$ and the spin-chirality fluctuations becomes gapless (i.e. Tomonaga-Luttinger like).

In the chirality-dominant phase $K_4 > J/2$ (or $\theta_{\text{sd}} < \theta < \pi/2$), ϕ is locked at $\phi = \pi/2, 3\pi/2$ and $\mathbf{\Omega} \sim (\mathbf{S}_1 \times \mathbf{S}_2)_{k=\pi}$.

This short-range vector-chiral fluctuations at $k = \pi$ are governed by the non-linear sigma model (A12) with

$$\chi_s = \frac{8K_4 - J}{2a(4K_4 - J)(4K_4 + J)}, \quad \rho_s = \frac{(8K_4 - J)(8K_4 + J)a}{64K_4}, \quad (\text{A14a})$$

$$\chi_c = \frac{1}{16aK_4}, \quad \rho_c = \frac{(8K_4 - J)(8K_4 + J)a}{64K_4}, \quad (\text{A14b})$$

$$g(J, K_4) = -\frac{(2K_4 - J)(8K_4 - J)(8K_4 + J)}{256K_4^2 a} (< 0). \quad (\text{A14c})$$

In deriving the effective model for the F-nematic phase realized for $J + 2K_4 < 0$, we use another parametrization (50) which takes into account the transverse soft modes at $k = 0$

and the staggered U(1)-symmetry for $J + 2K_4 = 0$:

$$\mathbf{A}_r + i\mathbf{B}_r = \sqrt{\rho_0^2 + a l_\phi(x)} e^{(-1)^r i\phi(x)} \times \left\{ \sqrt{1 - a^2 \mathbf{l}_\Omega^2(x)} \boldsymbol{\Omega}(x) + ia(\boldsymbol{\Omega} \times \mathbf{l}_\Omega) \right\}, \quad (\text{A15})$$

where the two phenomenological parameters are now given by:

$$\chi_s = \frac{3J - 4K_4}{2a(J^2 + 4K_4J - 8K_4^2)}, \quad \rho_s = -\frac{J(J - 4K_4)(3J - 4K_4)a}{8(J - 2K_4)^2}. \quad (\text{A16a})$$

$$\chi_c = \frac{1}{4a(2K_4 - J)}, \quad \rho_c = \frac{a(-J)(4K_4 - J)(4K_4 - 3J)}{8(J - 2K_4)^2}, \quad (\text{A16b})$$

$$g(J, K_4) = -\frac{(J + 2K_4)(4K_4 - J)(4K_4 - 3J)}{16a(J - 2K_4)^2} (> 0). \quad (\text{A16c})$$

-
- ¹ D. J. Thouless, Proc. Phys. Soc. London **86**, 893 (1965).
 - ² M. Takahashi, J. Phys. C: Solid State Physics **10**, 1289 (1977).
 - ³ A. MacDonald, S. Girvin, and D. Yoshioka, Phys. Rev. B **37**, 9753 (1988).
 - ⁴ M. Roger, J. H. Hetherington, and J. M. Delrieu, Rev. Mod. Phys. **55**, 1 (1983).
 - ⁵ H. Fukuyama, J. Phys. Soc. Jpn. **77**, 111013 (2008).
 - ⁶ S. Chakravarty, S. Kivelson, C. Nayak, and K. Voelker, Philosophical Magazine Part B **79**, 859 (1999).
 - ⁷ Y. Shimizu, K. Miyagawa, K. Kanoda, M. Maesato, and G. Saito, Phys. Rev. Lett. **91**, 107001 (2003); M. Yamashita, N. Nakata, Y. Senshu, M. Nagata, H. M. Yamamoto, R. Kato, T. Shibauchi, and Y. Matsuda, Science **328**, 1246 (2010).
 - ⁸ R. Coldea, S. M. Hayden, G. Aeppli, T. G. Perring, C. D. Frost, T. E. Mason, S.-W. Cheong, and Z. Fisk, Phys. Rev. Lett. **86**, 5377 (2001).
 - ⁹ S. Brehmer, H.-J. Mikeska, M. Muller, N. Nagaosa, and S. Uchida, Phys. Rev. B **60**, 329 (1999).
 - ¹⁰ M. Matsuda, K. Katsumata, R. S. Eccleston, S. Brehmer, and H.-J. Mikeska, Phys. Rev. B **62**, 8903 (2000).
 - ¹¹ T. S. Nunner, P. Brune, T. Kopp, M. Windt, and M. Grüninger, Phys. Rev. B **66**, 180404 (2002).
 - ¹² C. J. Calzado, C. de Graaf, E. Bordas, R. Caballol, and J.-P. Malrieu, Phys. Rev. B **67**, 132409 (2003).
 - ¹³ K. P. Schmidt and G. S. Uhrig, Mod. Phys. Lett. B **19**, 1179 (2005).
 - ¹⁴ S. Notbohm, P. Ribeiro, B. Lake, D. A. Tennant, K. P. Schmidt, G. S. Uhrig, C. Hess, R. Klingeler, G. Behr, B. Buchner, M. Reehuis, R. I. Bewley, C. D. Frost, P. Manuel, and R. S. Eccleston, Phys. Rev. Lett. **98**, 027403 (2007).
 - ¹⁵ E. Bordas, C. de Graaf, R. Caballol, and C. J. Calzado, Phys. Rev. B **71**, 045108 (2005).
 - ¹⁶ B. Lake, A. M. Tselik, S. Notbohm, D. Alan Tennant, T. G. Perring, M. Reehuis, C. Sekar, G. Krabbes, and B. Buchner, Nat Phys **6**, 50 (2010).
 - ¹⁷ Y. Mizuno, T. Tohyama, and S. Maekawa, J. Low Temp. Phys. **117**, 389 (1999), 10.1023/A:1022577918657.
 - ¹⁸ A. Läuchli, J. C. Domenge, C. Lhuillier, P. Sindzingre, and M. Troyer, Phys. Rev. Lett. **95**, 137206 (2005).
 - ¹⁹ N. Shannon, T. Momoi, and P. Sindzingre, Phys. Rev. Lett. **96**, 027213 (2006).
 - ²⁰ T. Momoi, P. Sindzingre, and N. Shannon, Phys. Rev. Lett. **97**, 257204 (2006).
 - ²¹ T. Senthil, A. Vishwanath, L. Balents, S. Sachdev, and M. P. A. Fisher, Science **303**, 1490 (2004); S. S. A. V. T. Senthil, Leon Balents and M. Fisher, Phys. Rev. B **70**, 144407 (2004).
 - ²² A. W. Sandvik, Phys. Rev. Lett. **98**, 227202 (2007); Phys. Rev. Lett. **104**, 177201 (2010).
 - ²³ D. N. Sheng, O. I. Motrunich, and M. P. A. Fisher, Phys. Rev. B **79**, 205112 (2009); M. S. Block, R. V. Mishmash, R. K. Kaul, D. N. Sheng, O. I. Motrunich, and M. P. A. Fisher, Phys. Rev. Lett. **106**, 046402 (2011).
 - ²⁴ G. Misguich, B. Bernu, C. Lhuillier, and C. Waldtmann, Phys. Rev. Lett. **81**, 1098 (1998).
 - ²⁵ M. Freedman, C. Nayak, and K. Shtengel, Phys. Rev. Lett. **94**, 066401 (2005).
 - ²⁶ M. Müller, T. Vekua, and H.-J. Mikeska, Phys. Rev. B **66**, 134423 (2002).
 - ²⁷ A. Läuchli, G. Schmid, and M. Troyer, Phys. Rev. B **67**, 100409 (2003).
 - ²⁸ T. Hikihara, T. Momoi, and X. Hu, Phys. Rev. Lett. **90**, 087204 (2003).
 - ²⁹ T. Momoi, T. Hikihara, M. Nakamura, and X. Hu, Phys. Rev. B **67**, 174410 (2003).
 - ³⁰ V. Gritsev, B. Normand, and D. Baeriswyl, Phys. Rev. B **69**, 094431 (2004).
 - ³¹ K. P. Schmidt, H. Monien, and G. S. Uhrig, Phys. Rev. B **67**, 184413 (2003).
 - ³² T. Hakobyan, Phys. Rev. B **78**, 012407 (2008).
 - ³³ S. Nishimoto and M. Arikawa, Phys. Rev. B **79**, 113106 (2009).

- ³⁴ K. Hijii, S. Qin, and K. Nomura, Phys. Rev. B **68**, 134403 (2003).
- ³⁵ P. Lecheminant and K. Totsuka, Phys. Rev. B **71**, 020407 (2005).
- ³⁶ P. Lecheminant and K. Totsuka, Phys. Rev. B **74**, 224426 (2006).
- ³⁷ J.-L. Song, S.-J. Gu, and H.-Q. Lin, Phys. Rev. B **74**, 155119 (2006).
- ³⁸ I. Maruyama, T. Hirano, and Y. Hatsugai, Phys. Rev. B **79**, 115107 (2009); M. Arikawa, S. Tanaya, I. Maruyama, and Y. Hatsugai, Phys. Rev. B **79**, 205107 (2009).
- ³⁹ S.-H. Li, Q.-Q. Shi, J.-H. Liu, , and H.-Q. Zhou, “Ground-state fidelity and quantum criticality in a two-leg ladder with cyclic four-spin exchange,” ArXiv 1105.3276.
- ⁴⁰ S. Sachdev and R. N. Bhatt, Phys. Rev. B **41**, 9323 (1990).
- ⁴¹ A. K. Kolezhuk, Phys. Rev. Lett. **99**, 020405 (2007).
- ⁴² M. Sato, Phys. Rev. B **76**, 054427 (2007).
- ⁴³ T.-L. Ho, Phys. Rev. Lett. **81**, 742 (1998); T. Ohmi and K. Machida, J. Phys. Soc. Jpn. **67**, 1822 (1998); A. Imambekov, M. Lukin, and E. Demler, Phys. Rev. A **68**, 063602 (2003).
- ⁴⁴ A. K. Kolezhuk, Phys. Rev. B **53**, 318 (1996).
- ⁴⁵ A. Auerbach, *Interacting Electrons and Quantum Magnetism* (Springer-Verlag, 1994).
- ⁴⁶ X. G. Wen, *Quantum Field Theory of Many-Body Systems* (Oxford University Press, 2004).
- ⁴⁷ A. Andreev and I. Grishchuk, Sov.Phys. JETP **60**, 267 (1985).
- ⁴⁸ K. Totsuka, S. Capponi, and P. Lecheminant, In preparation.
- ⁴⁹ E. Demler and F. Zhou, Phys. Rev. Lett. **88**, 163001 (2002); F. Zhou, Int. J. Mod. Phys. B **17**, 2643 (2003).
- ⁵⁰ F. H. L. Essler, G. V. Shlyapnikov, and A. M. Tsvelik, J. Stat. Mech.: Theory and Experiment **2009**, P02027 (2009).
- ⁵¹ A. B. Zamolodchikov and A. B. Zamolodchikov, Annals of Physics **120**, 253 (1979).
- ⁵² D. Sénéchal, Phys. Rev. B **52**, 15319 (1995); G. Sierra, J. Phys. A: Mathematical and General **29**, 3299 (1996).
- ⁵³ The explicit form of the normal modes around $k = \pi$ shows that the corresponding fluctuation is of the form $\mathbf{A} \mapsto e^{i\delta\phi} \mathbf{A}$.
- ⁵⁴ T. Hikihara and S. Yamamoto, J. Phys. Soc. Jpn. **77**, 014709 (2008).
- ⁵⁵ In 1D, the projection of \mathbf{B} onto the plane perpendicular to H cannot order and only the z -component takes a finite expectation value; in higher dimension, on the other hand, it is possible that both \mathbf{A} and \mathbf{B} exhibit long-range order.
- ⁵⁶ T. Sakai and Y. Hasegawa, Phys. Rev. B **60**, 48 (1999); A. Nakasu, K. Totsuka, Y. Hasegawa, K. Okamoto, and T. Sakai, J. Phys.: Condensed Matter **13**, 7421 (2001).
- ⁵⁷ J. Romhányi, K. Totsuka, and K. Penc, Phys. Rev. B **83**, 024413 (2011).
- ⁵⁸ S. R. White, Phys. Rev. Lett. **69**, 2863 (1992).
- ⁵⁹ F. D. M. Haldane, Phys. Rev. Lett. **47**, 1840 (1981).
- ⁶⁰ After neglecting the longitudinal fluctuations, the charge part $\mathcal{H}_{\text{charge}}$ (28d) merely contributes a constant.